10th World Congress on Structural and Multidisciplinary Optimization
May 19 - 24, 2013, Orlando, Florida, USA

Topology Optimization for the Microstructure Design of Plasmonic Composites

Masaki Otomori[1], Jacob Andkjær[2], Ole Sigmund[3], Takayuki Yamada[4], Kazuhiro Izui[5], Shinji Nishiwaki[6]

[1] Kyoto University, Kyoto, Japan, otomori.masaki@gmail.com
[2] Technical University of Denmark, Lyngby, Denmark, jban@mek.dtu.dk
[3] Technical University of Denmark, Lyngby, Denmark, sigmund@mek.dtu.dk
[4] Kyoto University, Kyoto, Japan, takayuki@me.kyoto-u.ac.jp
[5] Kyoto University, Kyoto, Japan, izui@me.kyoto-u.ac.jp
[6] Kyoto University, Kyoto, Japan, shinji@prec.kyoto-u.ac.jp

1. Abstract
This paper presents a systematic methodology for the design of plasmonic composites such as silver-dielectric composites that exhibit extreme electric permittivity. A gradient-based topology optimization method is used to find the distribution of plasmonic material for the unit cell of a periodic microstructure composed of plasmonic and dielectric materials. The effective permittivity of plasmonic composites is obtained using energy-based homogenization. The finite element mesh is regenerated at every iteration during the optimization process so that the mesh accurately fits the zero iso-surface of the electric permittivity, to exactly express the interfaces between plasmonic and dielectric materials. Several numerical examples are provided to confirm the validity and utility of the presented method.
2. Keywords: Inverse homogenization, Topology optimization, Plasmonic material, Effective permittivity, Energy-based homogenization

3. Introduction

Composites with plasmonic inclusions such as silver-dielectric composites can exhibit extreme properties that dramatically enhance the capability and performance of optical devices such as a superlens [1], and optical nanocircuits [2]. For the design of such plasmonic composites, Wallen et al. [3,4] numerically investigated periodic silver-dielectric composites that demonstrate an effective permittivity of -1, for the design of a near-field superlens and composites that have extreme anisotropy. However, their designs were limited to simple inclusions, such as those with a low volume fraction circular shape, since their design method was based on mixing formulas [5] such as the Maxwell-Garnett mixing formula and the Rayleigh formula. To exploit the desirable properties of such composites materials to the full, a systematic design approach, such as the inverse homogenization method [6], is most efficient for designing the microstructure that forms the composite material. Inverse homogenization has been applied to many material property design problems, such as the design of materials with a negative thermal expansion coefficient [7], a negative Poisson's ratio [8], or desirable values of Young's modulus [6], magnetic permeability [9], or dielectric permittivity [10, 11]. In this study, a gradient-based topology optimization method is presented for the microstructure design of plasmonic two-phase composites that provide desired values of effective permittivity, including negative values.

Composite materials can be usually modeled as materials consisting of a periodic array of unit cells, and the effective properties of the overall structure can be computed using mixing formulas or homogenization methods. In this study, we use an energy-based homogenization method [12] that computes the effective properties based on the results of finite element analysis and can handle complicated inclusions in addition to the simple inclusions that classical mixing formulas can work with. The optimization problem is formulated as a problem to minimize the square of the difference between the effective permittivity and a prescribed value, or to minimize or maximize the effective permittivity when the design goal is to obtain extreme values. The optimization algorithm uses the adjoint variable method (AVM) for the sensitivity analysis and the finite element method (FEM) for solving the equilibrium and adjoint equations, respectively. A PDE-based filter [13, 14] and Heaviside function [15] are used to obtain clear optimized configurations and the method of moving asymptotes (MMA) [16] is used for updating design variables.

In plasmonic materials, due to surface plasmon resonance, the electric field is markedly enhanced at

the interface between the plasmonic and dielectric material, namely, the structural interfaces between the negative and positive permittivity materials. To appropriately capture this phenomenon, it is important to express these interfaces exactly, so the finite element mesh is regenerated at every iteration during the optimization process here so that the mesh accurately fits the zero iso-surface of the electric permittivity. Several design problems show that appropriate unit cell configurations that exhibit the prescribed electric permittivity can be obtained for isotropic and anisotropic design problems. The permittivity values obtained by the optimization are compared with theoretical bounds [17], such as Weiner's arithmetic means, harmonic means, and the Hashin-Strikman bound, and the results show that the values obtained by the proposed optimization method are in good agreement with these theoretical bounds. The design example for a near-field superlens is also presented.

First, the formulation of the homogenization method for obtaining the effective permittivity is described. The mesh regeneration scheme and the optimization problem for the design of plasmonic composites are then discussed. The numerical implementation based on the formulation of the optimization problem, which uses the FEM and AVM to compute the sensitivity are explained next. Finally, several numerical examples are provided to confirm the validity and utility of the presented method.

4. Formulation

4.1. Effective permittivity

An energy-based approach [6, 12] is employed here to compute the effective permittivity of the composite. The mutual energy accumulated in the original unit cell is given as

$$Q_{ij} = \frac{1}{2}\int_{\Omega} \varepsilon_r(\boldsymbol{x})\nabla\bar{\phi}_i \cdot \nabla\phi_j d\Omega, \tag{1}$$

where ε_r is the electric permittivity and ϕ_i represents the electric potential obtained when an electric voltage is applied in an x_i direction. $\boldsymbol{x}$ represents the coordinate in the unit cell, and $\bar{\phi}_i$ denotes the conjugate complex number of ϕ_i. The mutual energy accumulated in the homogenized cell is given as

$$Q_{ij}^H = \frac{1}{2}\varepsilon_{\text{eff},ij} V_i V_j V, \tag{2}$$

where V is the volume of the unit cell and V_i is the applied voltage in the x_i direction. By assuming the the mutual energies accumulated in the original unit cell Q_{ij}, and in the homogenized cell Q_{ij}^H are equivalent, the effective permittivities can be obtained as follows.

$$\varepsilon_{\text{eff,ij}} = \frac{1}{V_i V_j V}\int_{\Omega} \varepsilon_r\left(\boldsymbol{x}\right)\nabla\bar{\phi}_i \cdot \nabla\phi_j d\Omega. \tag{3}$$

4.2. Governing equation

Figure 1 shows the analysis domain and boundary conditions for a two-dimensional problem. The electric potentials, ϕ_i, used in the above formulation are obtained by solving the following governing equation.

$$\nabla \cdot \left(\varepsilon_r\left(\boldsymbol{x}\right)\nabla\phi_i\right) = 0. \tag{4}$$

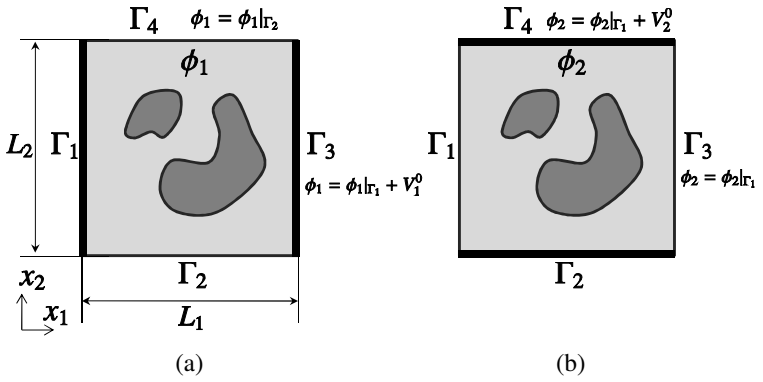

Figure 1: Analysis domain and boundary conditions when an electric voltage applied in (a) a horizontal direction, and (b) a vertical direction.

In the two-dimensional problem, ϕ_1 is obtained with the electric voltage applied in a horizontal direction, i.e., the x_1 direction. In this case, the left and right boundaries, and the upper and lower boundaries, respectively have the following periodic boundary conditions imposed [Fig.1(a)].

$$\phi_1(x,y) = \phi_1(x - l_1, y) + V_1 \quad \text{on} \quad \Gamma_3 \tag{5}$$
$$\phi_1(x,y) = \phi_1(x, y - l_2) \quad \text{on} \quad \Gamma_4, \tag{6}$$

where l_1, l_2 are the unit cell lengths in the x_1 and x_2 direction, respectively.

ϕ_2 is obtained with an electric voltage applied in a vertical direction, i.e., the x_2 direction. Here, the left and right boundaries, and the upper and lower boundaries, respectively have the following periodic boundary conditions imposed [Fig.1(b)].

$$\phi_2(x,y) = \phi_2(x - l_1, y) \quad \text{on} \quad \Gamma_3 \tag{7}$$
$$\phi_2(x,y) = \phi_2(x, y - l_2) + V_2 \quad \text{on} \quad \Gamma_4. \tag{8}$$

The effective permittivities are obtained by substituting the obtained electric potentials into Eq.(3).

4.3. Design variables

In this work, the relative electric permittivity ε_r inside the fixed design domain is defined using the relative element density $\tilde{\rho}$ based on the density approach.

$$\varepsilon_r = (\varepsilon_1 - \varepsilon_0)\,\tilde{\rho}^p + \varepsilon_0, \tag{9}$$

where ε_1 is the relative permittivity of the plasmonic material, ε_0 is the relative permittivity of the background material, and p is a penalization parameter.

To ensure that the optimal design is independent of the mesh, and to obtain a clear optimal configuration, a PDE-based filter [13, 14] and Heaviside function [15] are used in this work. Using this filter, the relative element densities $\tilde{\rho}$ can be computed as shown in the following procedures. First, intermediate variables μ are computed using following partial differential equation.

$$-R^2\nabla^2\mu + \mu = \rho, \tag{10}$$

where R represents filter radius. The relative element densities $\tilde{\rho}$ are then obtained using the Heaviside function [15] as follows.

$$\tilde{\rho} = \rho_{th}\left[e^{\beta(1-\mu/\rho_{th})} - (1-\mu/\rho_{th})e^{-\beta}\right] \quad (0 \le \mu < \rho_{th}) \tag{11}$$
$$\tilde{\rho} = (1-\rho_{th})\left[1 - e^{-\beta(\mu-\rho_{th})/(1-\rho_{th})} + (\mu-\rho_{th})e^{-\beta}/(1-\rho_{th})\right] + \rho_{th} \quad (\rho_{th} \le \mu < 1), \tag{12}$$

where β is a parameter that adjusts the curvature of the Heaviside function. ρ_{th} is a threshold value defined so that the corresponding relative element density $\tilde{\rho}$ has an electric permittivity value of zero. Namely,

$$\rho_{th} = \left(\frac{-\varepsilon_0}{\varepsilon_1 - \varepsilon_0}\right)^{1/p}. \tag{13}$$

4.4. Mesh regeneration procedure

In plasmonic materials, due to surface plasmon resonance, the electric field is markedly enhanced at the interface between the plasmonic and dielectric materials, namely, the structural interfaces between the materials that have negative or positive permittivity. To appropriately capture this phenomenon, it is important to express these interfaces exactly, so the finite element mesh is regenerated at every iteration during the optimization process here, to ensure that the mesh accurately fits the zero iso-surface of the electric permittivity. First, the iso-surface of intermediate variables μ that correspond to the zero iso-surface of the electric permittivity are computed as shown in Fig.2(a). The nodes that represents the zero iso-surface are extracted using the method in [18] which is used for the re-initialization scheme in level set-based topology optimization method. The finite element mesh regeneration is illustrated in Fig.2(b). The relative element densities $\tilde{\rho}$ are then obtained via the Heaviside function.

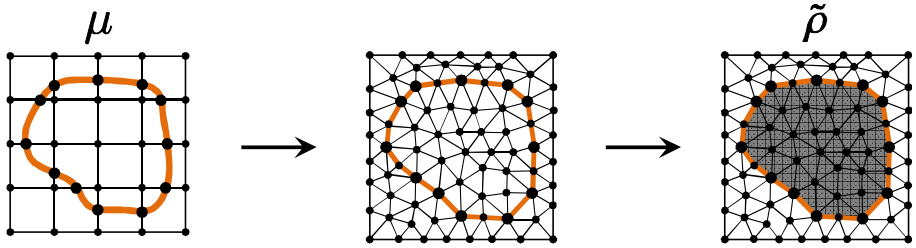

Figure 2: Remeshing procedure: (a)zero iso-surface of ε_r; (b) the finite element mesh is regenerated at every iteration so that the mesh accurately fits the zero iso-surface of ε_r; (c) $\tilde{\rho}$ is obtained via a Heaviside function.

4.5. Optimization problem

The purpose of the optimization is to obtain a microstructure design for plasmonic and dielectric materials that achieves the desired dielectric permittivity or extreme values of effective permittivity. The objective of the optimization problem can be formulated The optimization problem is formulated as follows.

$$\inf_{\rho} \qquad F = \log \sum_{ij} \varepsilon^*_{\mathrm{eff,ij}} \tag{14}$$

$$\text{subject to} \quad G = \frac{1}{V} \int_D \tilde{\rho} d\Omega - V_{\max} \leq 0 \tag{15}$$

$$\text{Governing equation} \tag{16}$$

$$\text{Boundary conditions} \tag{17}$$

The * represents the use of either $'$ or $''$ that applies to the real or imaginary part of the effective permittivity, respectively. The subscripts $ij = 11, 12, 21, 22$ denote the elements of the permittivity tensor, and $V_{\max}$ is the upper limit of the volume fraction.

5. Numerical implementation

Figure 3 shows the optimization flow chart. First, the design variables are initialized. Next, the intermediate variables μ are computed using the projection function. The finite element mesh is regenerated so that the mesh accurately fits the zero iso-surface of the electric permittivity. The objective and constraint functionals are then computed by solving the equilibrium equations using the FEM. If the objective functional has converged, the optimization procedure is terminated. If not, the sensitivities are computed using the AVM. The design variables ρ are then updated using the method of moving asymptotes (MMA) [16] and the process returns to the second step.

6. Numerical examples

Here, we present numerical examples to demonstrate the validity and capability of the presented method for the design of microstructures based on plasmonic and dielectric materials. The design domain is discretized using 25×25 square elements for the design variables ρ. A circular rod shape with a volume fraction of 50% is used as the initial configuration.

6.1. Designs targeting extreme values

Here we consider the design of composites that exhibit extreme values of effective permittivity. The relative permittivities of the plasmonic and dielectric materials are set to $\varepsilon_r = -4 + 4i$ and $\varepsilon_r = 1$. The maximum volume fraction is set to 60%.

Figure 4 shows the configurations obtained by the optimization. For the design of an anisotropic material, the real part of the effective permittivity $\mathrm{Re}(\varepsilon_{11})$ is minimized in Case1. For the design of isotropic materials, the real part of the effective permittivities $\mathrm{Re}(\varepsilon_{11})$ and $\mathrm{Re}(\varepsilon_{22})$ are minimized in Case2, and the real part of the effective permittivities $\mathrm{Re}(\varepsilon_{11})$ and $\mathrm{Re}(\varepsilon_{22})$ are maximized in Case3. The

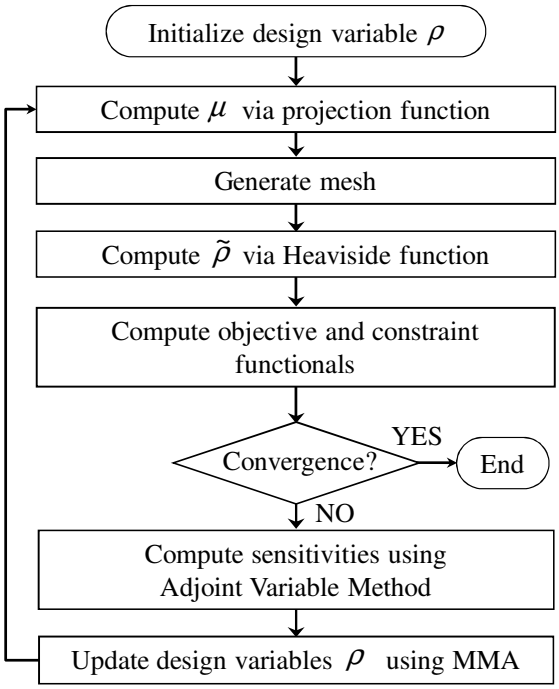

Figure 3: Flowchart of optimization algorithm

obtained effective permittivity in Case 1 is

$$\varepsilon_{\text{eff}} = \begin{bmatrix} -1.97 + 2.78i & 0.00 - 0.00i \\ 0.00 - 0.00i & 1.37 + 2.98 \end{bmatrix}, \tag{18}$$

the obtained effective permittivity in Case 2 is

$$\varepsilon_{\text{eff}} = \begin{bmatrix} -0.90 + 2.58i & 0.01 - 0.00i \\ 0.01 - 0.00i & -0.90 + 2.58i \end{bmatrix}, \tag{19}$$

and the obtained effective permittivity in Case 3 is

$$\varepsilon_{\text{eff}} = \begin{bmatrix} 0.27 + 3.93i & -0.01 + 0.00i \\ -0.01 + 0.00i & 0.25 + 3.94i \end{bmatrix}. \tag{20}$$

Figure 5 shows the finite element mesh of the obtained result in Case 3. It shows that the finite element mesh is generated to ensure that the mesh accurately fits the zero iso-surface of the electric permittivity.

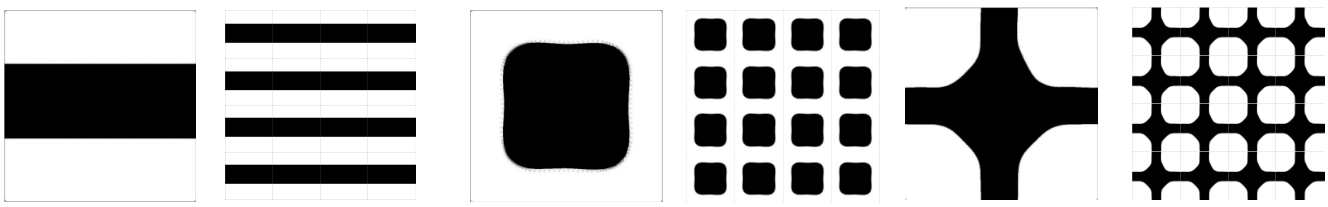

(a) (b) (c)

Figure 4: Obtained configurations and its layered structure: (a) Case1, minimizing $\text{Re}(\varepsilon_{11})$; (b) Case2, minimizing $\text{Re}(\varepsilon_{11}) + \text{Re}(\varepsilon_{22})$; (c) Case3, maximizing $\text{Re}(\varepsilon_{11}) + \text{Re}(\varepsilon_{22})$.

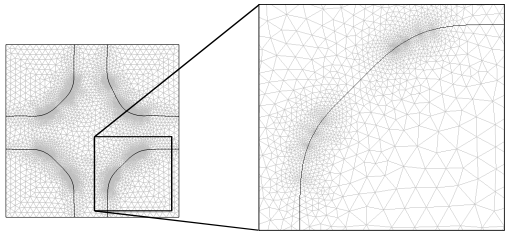

Figure 5: Finite element mesh of the obtained configuration (Case3).

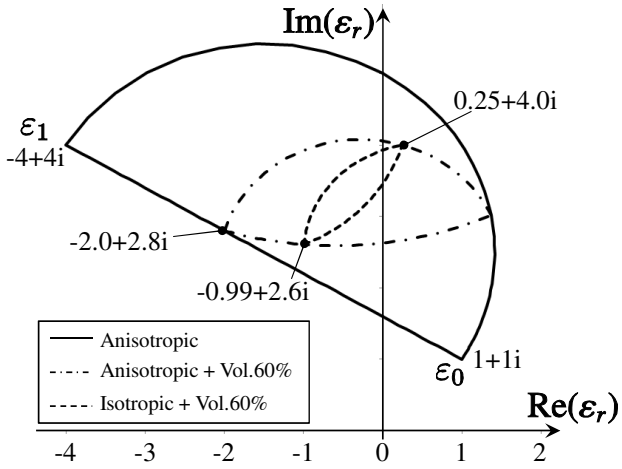

Figure 6: Theoretical bounds for anisotropic material (solid line) and anisotropic material with a volume fraction of 60% (dot-dashed line), and an isotropic material with a volume fraction of 60% (dashed line)

Figure 6 shows the theoretical bounds for anisotropic material (solid line), an anisotropic material with a volume fraction of 60% (dot-dashed line), and an isotropic material with a volume fraction of 60% (dashed line). The results show that the optimization successfully found designs that exhibit extreme effective permittivity values.

6.2. Near-field superlens design

A near-field superlens requires effective permittivity $\epsilon_{\text{eff}} = -1$, so we apply constraints to ensure that the real part of effective permittivities $\text{Re}(\epsilon_{11}) = \text{Re}(\epsilon_{22}) = -1$ and set the objective of optimization to minimize the loss, i.e., minimize $\text{Im}(\epsilon_{11}) + \text{Im}(\epsilon_{22})$. The relative permittivity of the plasmonic material is set to $\epsilon_r = -9.29 + 0.25i$, a value close to that for pure silver at wavelength $\lambda = 500$nm. The relative permittivity of the dielectric material is set to $\epsilon_r = 1$. The maximum volume fraction is set to 60%.

Figure 7 shows the obtained configuration for which the obtained effective permittivity is

$$\epsilon_{\text{eff}} = \begin{bmatrix} -1.00 & 0.065 \\ 0.065 & -1.01 \end{bmatrix}. \tag{21}$$

Here we confirm that the obtained configuration actually functions as a near-field superlens. Figure 8 shows the analysis model for the near-field superlens. TM polarized waves enter the domain at the left boundary. A plate with a single aperture is placed at $x = 0.0$ between upper and lower boundaries that have a periodic boundary condition imposed, and a composite near-field superlens consisting of 4×16 unit cells of the design obtained in the previous optimization in a periodic array is placed placed to the right side of the aperture plate. The thickness of the near field superlens is $d = \lambda/10$. Figure 9(a) shows the magnetic field distribution and Fig. 9(b) shows a plot of the magnetic field at $x = 0$ and $x = 2d$. The field results show that an image of the slit is reconstructed at the plane $x = 2d$.

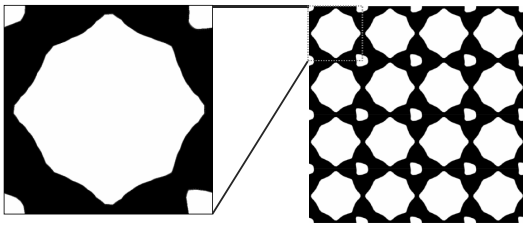

Figure 7: Obtained configuration.

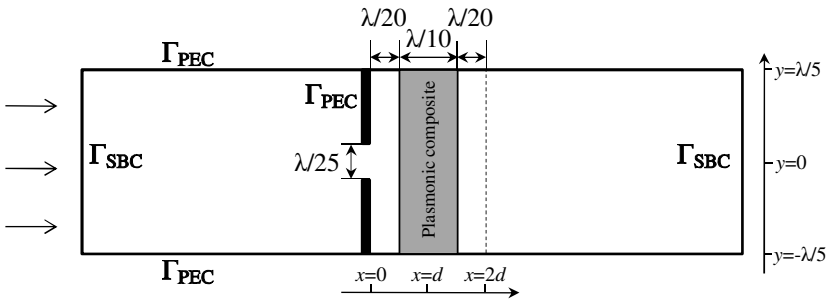

Figure 8: Numerical model for near-field superlens.

7. Conclusion

We presented a gradient-based topology optimization method for the microstructure design of plasmonic composites. An energy-based homogenization was applied to obtain the effective permittivity, and a mesh regeneration scheme was used to exactly express the interfaces between the plasmonic and dielectric materials, by regenerating the finite element mesh at every iteration during the optimization process, to ensure that the mesh accurately fits the zero iso-surface of the electric permittivity. Finally, several numerical examples were provided to confirm the validity and utility of the presented method. In future research, we hope to extend the presented scheme to design problems that include dynamic time variance.

8. Acknowledgements

The first author was partly supported by Aisin AW Co., Ltd., and sincerely appreciates this assistance.

9. References

[1] W. Cai, D. A. Genev and V. M. Shalaev, Superlens based on metal-dielectric composites, *Physical Review B*, 72, 193101, 2005.

[2] N. Engheta, Circuits with light at nanoscales: Optical nanocirciuts inspired by metamaterials, *Science,* 317, 1698-1702, 2007.

[3] H. Wallen, H. Kettunen and A. Sihvola, Mixing formulas and plasmonic composites, *Metamaterials and Plasmonics: Fundamentals, Modelling, Applications, NATO Science for Peace and Security Series B: Physics and Biophysics*, 10 (4), 91-102, 2009.

[4] H. Wallen, H. Kettunen and A. Sihvola, Composite near-field superlens design using mixing formulas and simulations, *Metamaterials*, 3 (3-4), 129-139, 2009.

[5] A. Sihvola, *Electromagnetic Mixing Formulas and Applicataions*, The Institution of Engineering and Technology, London, 1999.

[6] O. Sigmund, Materials with prescribed constitutive parameters: an inverse homogenization problem, *International Journal of Solids and Structures*, 31 (17), 2313-2329, 1994.

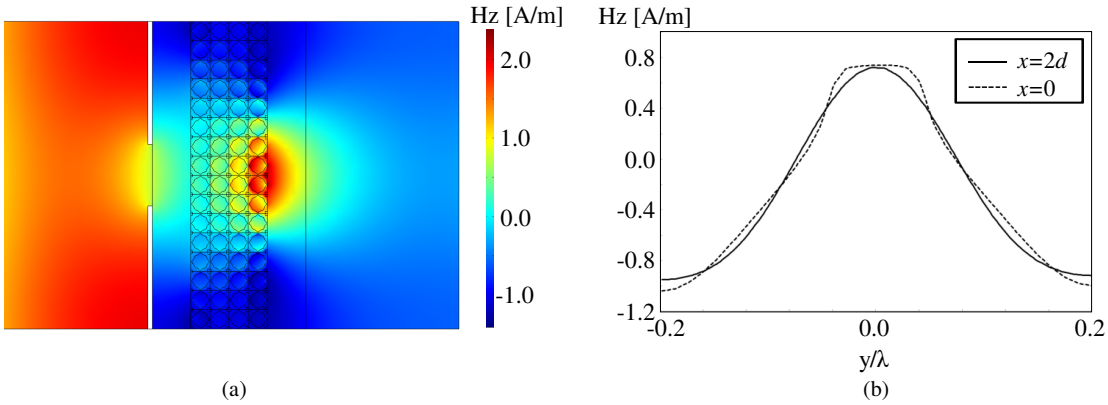

Figure 9: (a) magnetic field distribution; (b) plots of the magnetic field at $x = 0$ (dashed line) and $x = 2d$ (solid line).

[**7**] U. D. Larsen, O. Sigmund, and S. Bouwstra, Design and fabrication of compliant micromechanisms and structures with negative Poisson's ratio, *Journal of Microelectromechanical Systems*, 6 (2), 99-16, 1997.

[**8**] O. Sigmund and S. Torquato, Design of materials with extreme thermal expansion using a three-phase topology optimization method, *Journal of the Mechanics and Physics of Solids*, 45 (6), 1037-1067, 1997.

[**9**] J. S. Choi and J. Yoo, Design and application of layered composites with the prescribed magnetic permeability, *International Journal for Numerical Methods in Engineering*, 82 (1), 1-25, 2010.

[**10**] Y. El-Kahlout and G. Kiziltas, Inverse synthesis of electromagnetic materials using homogenization based topology optimization, *Progress in Electromagnetics Research*, 115, 343-380, 2011.

[**11**] M. Otomori, J. Andkjær, O. Sigmund, K. Izui and S. Nishiwaki, Inverse design of dielectric materials by topology optimization, *Progress in Electromagnetics Research*, 127, 93-120, 2012.

[**12**] Z. Hashin, Analysis of composite materials - a survey, *Journal of Applied Mechanics*, 50 (3), 481-505,1983.

[**13**] B. S. Lazarov and O. Sigmund, Filters in topology optimization based on Helmholtz-type differential equations, *International Journal for Numerical Methods in Engineering*, 86 (6), 765-781, 2011.

[**14**] A. Kawamoto, T. Matsumori, S. Yamasaki, T. Nomura, T. Kondoh and S. Nishiwaki, Heaviside projection based topology optimization by a PDE-filtered scalar function, *Structural and Multidisciplinary Optimization*, 44 (1), 19-24, 2011.

[**15**] S. Xu, Y. Cai and G. Cheng, Volume preserving nonlinear density filter based on heaviside functions, *Structural and Multidisciplinary Optimization*, 41 (4), 495-505, 2010.

[**16**] K. Svanberg, The method of moving asymptotes - a new method for structural optimization, *International Journal for Numerical Methods in Engineering*, 24 (2), 359-373, 1987.

[**17**] G. W. Milton, *The Theory of Composites*, Cambridge University Press, Cambridge, 2001.

[**18**] S. Yamasaki, S. Nishiwaki, T. Yamada, K. Izui and M. Yoshimura, A structural optimization method based on the level set method using a new geometry-based re-initialization scheme, *International Journal for Numerical Methods in Engineering*, 83 (12), 1580-1624, 2010.